Application Note

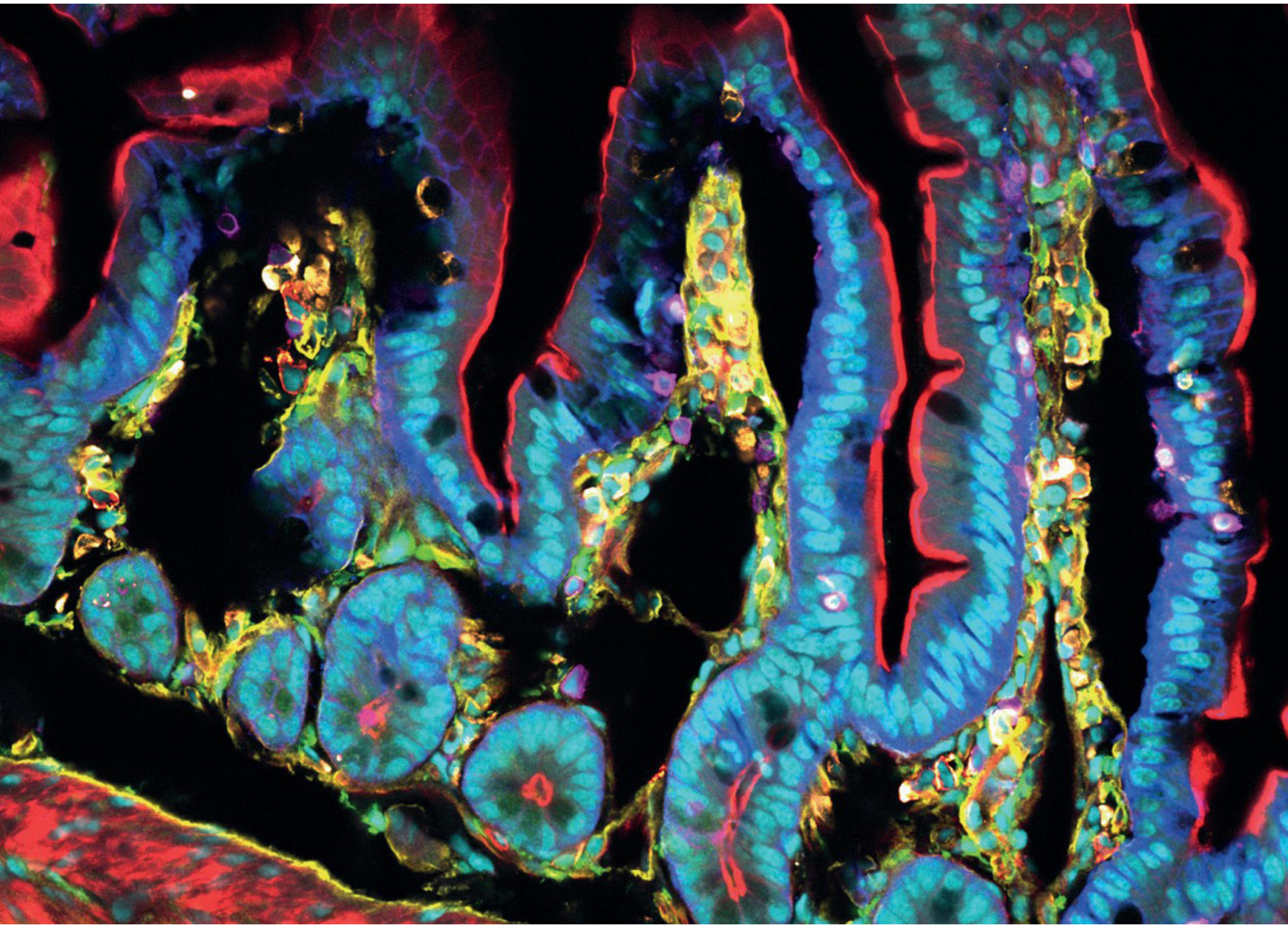

A Ten-color Spectral Imaging Strategy to Reveal Localization of Gut Immune Cell Subsets

A Ten-color Spectral Imaging Strategy to Reveal Localization of Gut Immune Cell Subsets

Authors: Hugues Lelouard, PhD, CR; Sébastien Mailfert, PhD, IR; Mathieu Fallet, IE
Aix-Marseille Université, Centre for Scientific Research (CNRS), Inserm, Centre d'immunologie de Marseille-Luminy, Marseille, France

Date: November 2018

Introduction

In immunology, recent progresses in multi-parametric and mass cytometry allowed the discovery of many discrete subsets or states of activation inside a single cell lineage population. The use of multiple antibodies labelled with different organic dyes or isotopes allows indeed the simultaneous detection of many different cell types or subsets extracted from a given organ [1] [2] [3]. Therefore, mass and flow cytometry represent invaluable tools with an impressive statistical relevance due to the simultaneous analyze of huge number of cells (thousands to millions) tagged with many different probes.

However, these techniques do not provide some key information, such as location of cells of interest inside the tissue and their interaction with other cells or components of the tissue remain unknown, as well as location of antigens on the surface (randomly distributed versus clustered in specific area, only present at the surface versus internalized). Modern microscopes can provide such qualitative information due to their accuracy in terms of resolution and sensitivity. The technique, which currently provides the highest sensitivity and resolution on the wider spectral range, is confocal microscopy. However, the number of fluorescent probes that can be distinguished in a classic channel-like acquisition is limited by spectral overlap and rarely exceeds 5 fluorochromes. The recent development of spectral imaging coupled to linear unmixing overcomes this limitation by resolving overlapping fluorescent spectra. In addition, many biological tissues contain autofluorescent constituents with large spectral dispersion that could affect the quality of the desired signal or could lower the signal-to-noise ratio (contrast). Spectral imaging can solve these autofluorescence background issues and even identify the autofluorescent compounds based on their emission spectra. Here, we propose a ten-color spectral imaging strategy that allows the localization of structural elements (collagen fibers, actin filaments, auto-fluorescent material), nuclei, gut epithelial cells and four immune cell types (B and T cells, dendritic cells and macrophages).

Experimental procedure

The biological protocol is summarized in the appendix. All the markers used in the present study are listed in table 1. Image acquisition was performed on a ZEISS LSM 780 confocal microscope equipped with a 405 nm diode laser, Argon (445 nm, 488 nm, 514 nm) and Helium Neon (561 nm, 633 nm) lasers. The gallium arsenide phosphide (GaAsP) spectral array detector was tuned to 8.9 nm to obtain 32 channel images ranging from 414 to 690 nm (figure 2) from which emission spectrum for each fluorochrome was extracted and used in the "online fingerprinting" mode of imaging software ZEN (black edition). We used a Plan-Apochromat 40×/1.4 Oil DIC M27 objective lens, a pinhole size of one Airy unit and a pixel dwell time of 3.15 µs.

Results

Staining precautions

In order to avoid any possible spectral attribution mistake during the linear unmixing process, we decided first to use as much as possible spectrally separated dyes and second to avoid fluorochromes with close emission spectra for antigens with strong localization overlap.

	Marker	Source	Description	Detection method
Cells	Rat anti-EpCAM (clone G8.8)	ThermoFisher	Detection of a cell adhesion molecule specific of the epithelium; expressed by the plasma membrane of all gut epithelial cells	Coupled to eFluor 450
	Chicken Anti-GFP	Aves Labs	Detection of the GFP, i.e. CX3CR1 expression, i.e. monocyte-derived cells	Donkey anti-chicken-Alexa Fluor 488
	Rat anti-CD45R (clone RA3-6B2)	Biolegend	Detection of a protein tyrosine phosphatase mainly expressed by B cells	Donkey anti-rat-Cy3
	Hamster anti-CD11c (clone N418)	Biolegend	Detection of the alpha X integrin mainly ex-pressed by dendritic cells and macrophages	Goat anti-armenian hamster-Alexa Fluor 594
	Rat anti-CD3 (clone 145-2C11)	ThermoFisher	Specific marker of T cells	Coupled to eFluor 660
Morphology	UEA-I lectin	Vector Laboratories	Detection of α-fucosylated carbohydrates; mainly expressed in the granules of Paneth cells of the villous crypts and in the mucus	Coupled to Biotin + Streptavidin-Alexa Fluor 405
	SYTOX Blue	ThermoFisher	Nucleic acid stain; nucleus labeling	Added to the mounting medium
	Rabbit anti-collagen IV	Abcam	Detection of a major component of reticular fibers, collagen	Goat anti-rabbit-Alexa Fluor 514
	Phalloidin	ThermoFisher	Detection of filamentous actin. Enriched in the apical membrane of enterocytes (brush border)	Coupled to Alexa Fluor 660
	Auto-fluorescence	–	Mainly present at the level of the epithelium and in some macrophages	–

Table 1 *Description of the markers used in the study*

a)

	Ex (nm)	Em (nm)	E ($cm^{-1}M^{-1}$)	Quantum yield	Brightness	Coupled element	Source
Alexa Fluor 405	401	421	34 000	-	-	Streptavidin	ThermoFisher
eFluor 450	405	446	-	-	-	Rat anti-EpCAM	ThermoFisher
SYTOX Blue	444	480	-	-	-	None	Thermofisher
Alexa Fluor 488	495	519	71 000	0.94	66 740	Donkey anti-chicken	ThermoFisher
Alexa Fluor 514	517	542	80 000	0.1	8 000	Goat anti-rabbit	ThermoFisher
Cy3	554	568	150 000	0.15	22 500	Donkey anti-rat	Jackson ImmunoResearch
Alexa Fluor 594	590	617	73 000	0.64	46 720	Goat anti-hamster	ThermoFisher
eFluor 660	651	669	-	-	-	Rat anti-CD3	ThermoFisher
Alexa Fluor 660	663	690	132 000	0.37	48 840	Phalloidin	ThermoFisher

b)

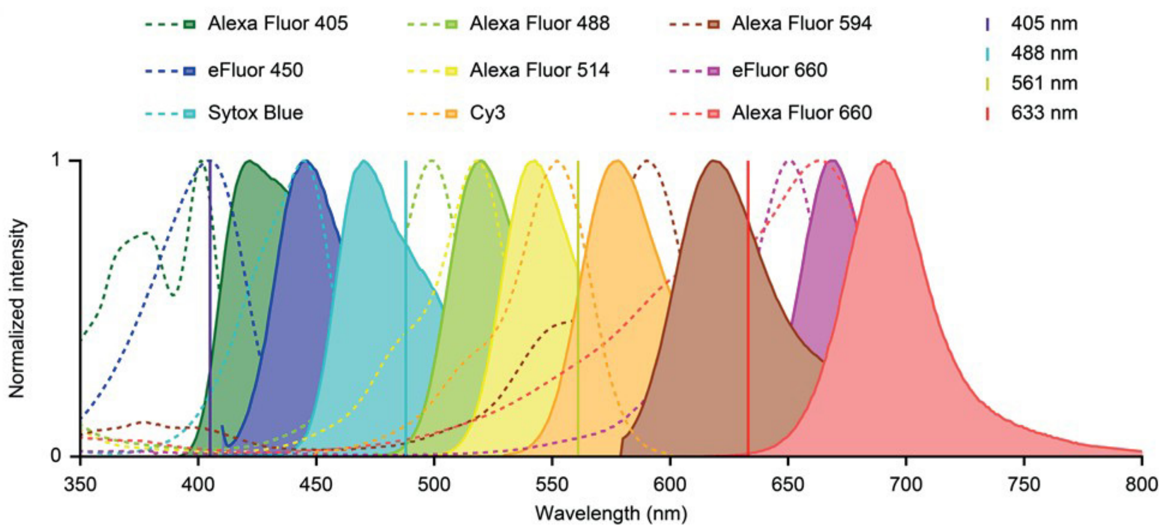

Figure 1 *(a) Characteristics [5] [6] and (b) excitation and emission spectra of the fluorochromes used in the study. Dashed lines corresponds to the excitation spectra and filled curves to the emission spectra, – denotes unavailable data.*

Choice of acquisition parameters
Acquired spectra contain rejection bands due to the presence of dichroic mirrors in the optical path corresponding to laser excitation wavelengths. This may interfere with good detection of emission signals. Dichroic mirror effect is shown in figure 2a. In this lambda mode gallery the 485 nm signal of the Alexa Fluor 405 emission is lost due to the main beam splitter MBS 488/561/633. Thus, we decided to use the lowest number of laser lines necessary to acquire all fluorochromes, i.e. 405, 488, 561 and 633 nm, even if some fluorochromes were not optimally excited (e.g. the nucleic acid stain SYTOX Blue and Alexa Fluor 514; figure 1).

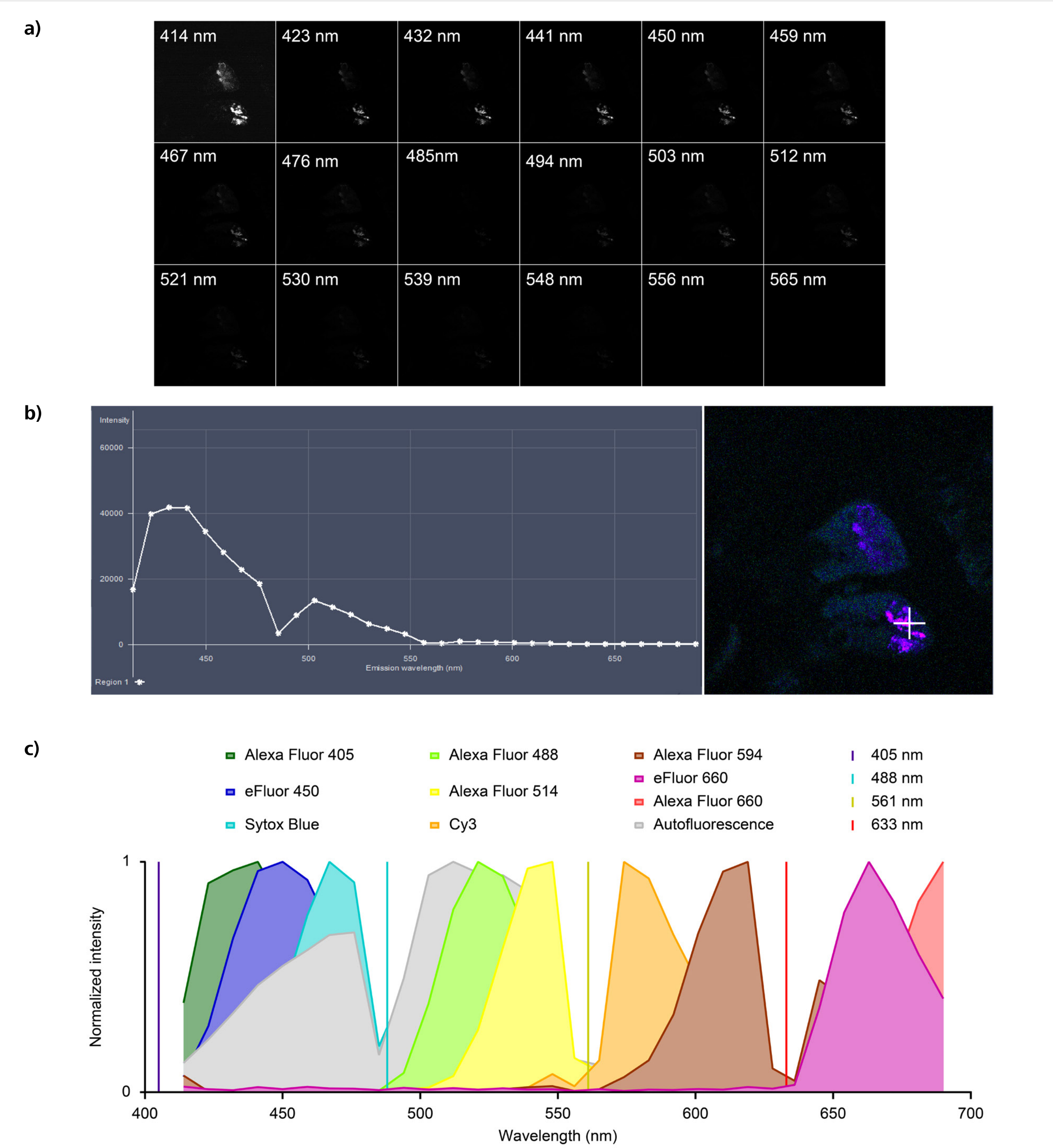

Figure 2 *(a) Gallery view of the 18 first channel (over 32) images ranging from 414 to 585 nm acquired in the lambda mode for Alexa Fluor 405*
(b) Left: Alexa Fluor 405 spectrum corresponding to the white cross displayed on the lambda color-coded image (right)
(c) Emission spectrum of the 10 fluorescent signals used in the study (9 fluorochromes and one autofluorescence)

Reference emission spectrum acquisition

Individual emission spectrum acquisition was conducted with the "lambda" mode of the imaging software ZEN (black edition). To optimize the signal-to-noise ratio of the spectrum, the master gain of the GaAsP spectral array detector was maintained under 700 with an averaging of four images. We recommend acquiring each individual reference spectrum on mono-labelled samples. When this is impossible (e.g. constitutive expression of fluorescent proteins or strong auto-fluorescence), spatial location of each fluorochrome has to be well characterized in order to define region of interest (ROI) containing only one fluorochrome in the wavelength color-coded look-up table (LUT) of the "unmixing" tab panel (figure 2b). The emission spectrum of the fluorochrome located in the ROI is automatically displayed (figure 2b). Representativeness of the spectrum can be assessed by moving the ROI in the LUT image. The larger the ROI, the smoother the spectrum is but care has to be taken not to include other fluorescence signals in the ROI. The 10 reference spectra are shown in figure 2c (9 fluorochromes and 1 autofluorescence).

Brightness adjustment

A major issue came from the fact that a unique master gain tunes the amplification of the GaAsP spectral array detector, in order to provide unchanged spectral information. This means that fluorochromes excited by the same laser are detected with the same level of amplification. Thus, staining conditions should be optimized to obtain emitted signals as close as possible from each other. It is then possible in the online fingerprinting mode to adjust the brightness of the individual channels by increasing slightly the digital gain. Value of the latter should however be kept lower than 2 to keep a good sig-

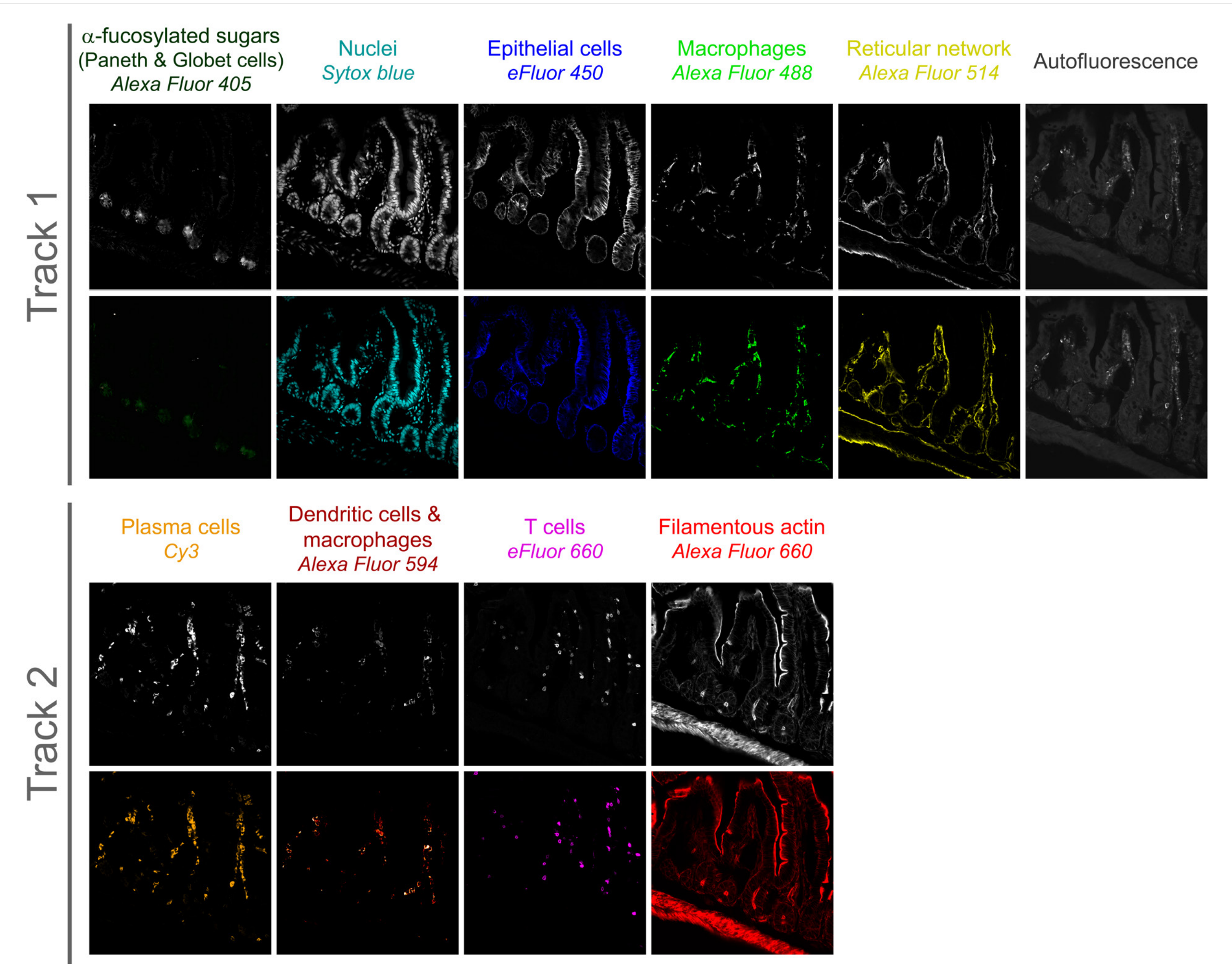

Figure 3 *Online fingerprinting images of track 1 (upper panel) generated with the 405 & 488 nm excitation wavelength and track 2 (lower panel) generated with the 561 & 633 nm excitation wavelength. B&W and pseudo-color images are displayed for each fluorochrome for better visualization of the signal contrast.*

nal-to-noise ratio. Finally, in the same tissue, antigens may be expressed at different levels depending on cells or location. This can lead to an unsolved issue where emitted signal amplitude is too broad to avoid saturation without losing information on the weakly fluorescent part of the acquired data.

Two tracks for a 10 color experiment
Contrary to the post processing function for the linear unmixing, in the "online fingerprinting" mode, it is currently not possible to run simultaneously more than eight channels, i.e. eight spectra. Thus, we had to separate acquisitions of the different fluorochromes into two tracks using the "experiment designer" module. We imaged separately the dyes into two tracks. The first track contained the auto-fluorescence channel as well as five fluorochromes excited by the 405 nm diode laser and by the 488 nm line of the argon laser. The second track contained four fluorochromes excited at 561 and 633 nm. Figure 3 shows the unmixed images acquired into both tracks. For our biological aim, the autofluorescence does not reveal a signal of interest except to visualize the contour of the tissue / organ. The critical point is to be sure to separate accurately the 9 other channels which reveal the signature of each individual cell type and its localization within the tissue. Results are displayed in figure 4 with track 1, track 2 and the merged image. We also showed two images corresponding to the cells & the "morphology" of the tissue (right top corner).

Discussion and troubleshooting

Spectrum purity – Spectral imaging requires that separated spectra are distinguishable from the others, and are linearly independent meaning than none of the spectra can be written as a linear combination of the others. The consequence is that the characterization of each pure (reference) spectrum is important. Otherwise, this could lead to the appearance of artifacts like crosstalk. Moreover, the reference spectrum should be defined with the minimum of noise to avoid signal loss.

Blind or supervised emission spectrum extraction – The ACE mode (Automatic Component Extraction) is an unsupervized mode based on principal component analysis [7] to find the spectrum without sample controls. It works pretty well if it is possible to find a pure spectrum in the lambda images. Practically, the algorithm is looking for regions of bright intensities and could focalize unfortunately on non-representative details. A manual checking is then mandatory to check the proposed solution provided by the software.

Emission spectrum dependence on laser power – Once the reference spectrum is recorded, the signal could be adjusted in terms of laser power, gain and digital gain. However, some fluorochromes or autofluorescence could be excited with different lasers. Moreover, autofluorescence is often the fruit of different compounds, making emission spectrum characterization more complex. In all these cases, the total spectrum could depend on the ratio of laser power, which makes accurate unmixing trickier to obtain.

Saturated signal artifacts – Unfortunately, saturation of emission signal in one of the channels can lead to artifacts in the online unmixing process resulting in unspecific pixels in all channels. Therefore, detected signals should be kept as unsaturated as possible.

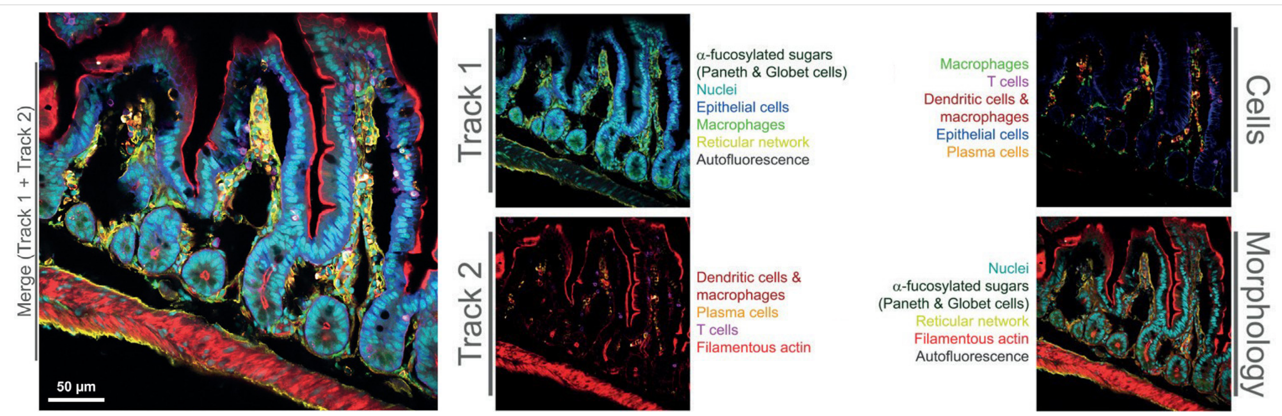

Figure 4 *Track 1, track 2 and the merged image. On the upper right corner, images emphasizing either cells or morphology of the tissue are displayed.*

Brightness ratio – brightness difference between fluorochromes can be an issue especially when they cannot be tunable. For example, CFP and GFP could be theoretically easily separated but this is not the case when the CFP/GFP brightness ratio is too high.

Dependency on the acquisition parameters – It is sometimes difficult to acquire a precise reference spectrum. A spectrum could depend on the z-position in a thick sample and the localization and size of the ROI. We have for example noticed that the DAPI spectrum could vary depending on these parameters. The presence of other staining in the preparation could of course be a reason of contamination by out of focus signal. Moreover, shorter wavelength light is more absorbed in depth. Finally, DAPI is also known to bind RNA with an emission shifted to around 500 nm when bound to RNA as compared to 460 nm for DNA [8].

Objective lens – Acquired spectra are usually valid only for one objective and a set of dichroic mirrors, i.e. the optical configuration of the experiment. Do not use reference spectra in other setting conditions. Spectrum differences between two objectives are strongly due to the UV transmission of objectives; e.g., the Plan-Apochromat 20×/0.8 has a better transmission at 450 nm than the Plan-Apochromat 40×/1.4 oil immersion objective.

Reproducibility – Detector aging could change the shape of the spectrum, so caution have to be taken when using old reference spectra.

Data rendering – The presentation of a ten-channel image is complex in term of color visualization and color handling. In an open source software like Image J, a maximum of 6 channels can be use.

Artefacts – We sometimes observe phenomena that we do not completely understand depending on the sample preparation like signal at shorter wavelength than the laser excitation that could be interpreted as anti-stokes emission or reflection on collagen fibers.

Conclusion

Spectral imaging is a powerful technique. Development of multi channel GaAsP detectors and live spectral unmixing algorithms enables very sensitive acquisition and easy experimental design. Recently, this multicolor imaging method has been successfully used to highlight the location of the different phagocyte subsets in mouse Peyer's patch [9] but it can also be useful in studies that include overlapping spectra such as FRET experiments or GFP/YFP mixed expression [10]. Finally, it is a powerful tool for autofluorescence studies or for imaging strongly autofluorescent tissue or cells without losing specific signal attribution [11].

Appendix

The CX3CR1-GFP ± transgenic mouse model was used [4]. Expression of the fluorescent protein GFP in place of the CX3CR1 gene allows the detection of all monocyte-derived cells present in the studied tissue (table 1). Permeabilization and saturation of unspecific binding sites were performed with PBS containing 0.5 % saponin, 1 % FCS, 1 % BSA, and 1 % of the secondary antibody species serum for 30 minutes before adding the mix of primary antibodies diluted in the same buffer. After overnight incubation with the primary antibodies at 4 °C, the tissue sections were washed in PBS and incubated with secondary antibodies for one hour. After washing, tissue sections were blocked with 1 % rat serum to allow the use of rat fluorochrome-coupled antibodies. Tissue sections were incubated with the latter for one hour before washing and mounting in Prolong Gold mounting medium (ThermoFisher) containing 0.1 % Sytox Blue (ThermoFisher) to stain nuclei.

About the authors

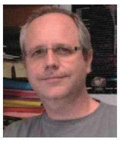

Hugues Lelouard is a CNRS researcher working in J.-P. Gorvel's team since 2007. His main research interests are to characterize the interactions between immune cells and enteropathogens in the small intestine and to elucidate the role of Peyer's patch phagocytes in mucosal immunity and gut homeostasis. Contact: lelouard@ciml.univ-mrs.fr

Sébastien Mailfert joined the H.-T. He and D. Marguet's team in 2007. He is in charge of the ImagImm platform facility and maintains the optical setups at the state of the art level with expertise in electronics, optics and software developments. He is studying the lateral membrane organization in living cells through svFCS and dSTORM techniques developed in the laboratory. Contact: mailfert@ciml.univ-mrs.fr

Mathieu Fallet joined the microscopy facility of the CIML in 2002. He is in charge of the ImagImm platform facility and maintains the optical setups at the state of the art level with an expertise in data analysis and image processing.
Contact: fallet@ciml.univ-mrs.fr

Founded in 1976, the Centre d'Immunologie de Marseille-Luminy is a research institute internationally renowned in its discipline which has developed an organization and practices designed to foster the creativity and risk-taking of its researchers. From worm to man, from molecules to the whole organism, from physiology to pathology the CIML addresses all areas of contemporary immunology, on many models and at various scales. These include the genesis of numerous cell populations, their modes of differentiation and activation, their implication in cancers, infectious and inflammatory diseases, and the mechanisms of cell death.

The Imaging Immunity – ImagImm - facility offers resources in photonic microscopy to decipher the operating mechanisms of the immune system, from molecules to whole organisms. The aims of the service are to: (1) develop microscopy methods at the state-of the-art, (2) provide scientific and technical assistance to acquire and analyze data, (3) train users with theoretical & practical courses, (4) maintain instruments and ensure quality control processes and (5) perform R&D activity for operating new biophotonic methods. ImagImm is member of the PICsL microscopy core facility, is identified at the national level as "Infrastructure en Biologie Santé et Agronomie" (IBISA) and is part of the France BioImaging network.

We acknowledge financial support from n° ANR-10-INBS-04-01 France Bio Imaging. HL designed the experiment, prepared the sample. HL, SM and MF acquired the data. HL, SM and MF wrote the application note.

References:

[1] Perfetto, «Seventeen-colour flow cytometry: unravelling the immune system,» Nat. Rev. Immunol., pp. 648–655, 2004.

[2] Bandura, «Mass Cytometry: Technique for Real Time Single Cell Multitarget Immunoassay Based on Inductively Coupled Plasma Time-of-Flight Mass Spectrometry,» Anal. Chem., pp. 6813–6822, 2009.

[3] Bendall, «Single-cell mass cytometry of differential immune and drug responses across a human hematopoietic continuum,» Science, pp. 687–696, 2011.

[4] J. Steffen, «Analysis of Fractalkine Receptor CX3CR1 Function by Targeted Deletion and Green Fluorescent Protein Reporter Gene Insertion,» Mol Cell Biol, pp. 4106–4114, 2000.

[5] cincinnatichildrens, «Fluorochromes brightness chart,» [Online]. Available: https://www.cincinnati- childrens.org/-/media/cincinnati%20 childrens/home/research/cores/flow cytometry/resources/related-ar- ticle1-pdf-fluorochrome%20brightness%20chart.pdf?la=en.

[6] Olympus Corportation, «Fluorochrome Data Table,» [Online]. Available: http://fluoview.magnet.fsu.edu/ theory/fluorochromedata.html.

[7] Garini, «Spectral imaging: principles and applications,» Cytometry Part A, vol. 69A, pp. 735–747, 2006.

[8] Kapuscinski, «Interactions of nucleic acids with fluorescent dyes: spectral properties of condensed com- plexes,» The journal of histochemistry and cytochemistry, pp. 1323–1329, 119.

[9] Bonnardel, «Distribution, location, and transcriptional profile of Peyer's patch conventional DC subsets at steady state and under TLR7 ligand stimulation,» Mucosal Immunol., pp. 1412–1430, 2017.

[10] Trompier, «Transition from Dimers to Higher Oligomeric Forms Occurs during the ATPase Cycle of the ABCA1,» Transporter journal of biological chemistry, 2006.

[11] Rommelaere, «Serum Pantetheinase/Vanin Levels Regulate Erythrocyte Homeostatis and Severity of Malaria,» The american journal of pathology, vol. 185, no. 11, 2015.

Carl Zeiss Microscopy GmbH
07745 Jena, Germany
microscopy@zeiss.com
www.zeiss.com/microscopy